A fast, high-throughput digital coincidence detection system for a large RPC-PET camera

PUBLISHED BY IOP PUBLISHING FOR SISSA MEDIALAB

RECEIVED: *September 30, 2012*
ACCEPTED: *January 22, 2013*
PUBLISHED: *March 1, 2013*

14th INTERNATIONAL WORKSHOP ON RADIATION IMAGING DETECTORS,
1–5 JULY 2012,
FIGUEIRA DA FOZ, PORTUGAL

A fast, high-throughput digital coincidence detection system for a large RPC-PET camera

F.M.C. Clemêncio,[a,1] **C.F.M. Loureiro**[b] **and J. Landeck**[b]

[a] *Escola Superior de Tecnologia da Saúde do Porto,*
Rua João de Oliveira Ramos, 87, 4000-294 Porto, Portugal
[b] *Department of Physics, University of Coimbra,*
P-3004-516 Coimbra, Portugal

E-mail: fcc@estsp.ipp.pt

ABSTRACT: Current work aiming at studying the feasibility of a resistive plate chamber (RPC)-PET camera for human whole-body screening indicates that a very cost-effective and high-sensitivity camera can be built. Such a camera will use the high intrinsic time resolution (better than 300 ps full width at half maximum (FWHM) of the RPC technology to implement a time of flight (TOF)-PET camera that, along with its very large field of view, can reach a sensitivity exceeding the present crystal-based PET technology by a factor up to 20 with a spatial resolution near 2 mm.

Due to the large number of RPC plates forming such a system (in the order of 100 RPC plates, or even more) and to the large amount of data generated it is essential to have an effective on-line trigger that helps reducing the pressure on the data saving and processing system.

In this work we present simulation results of an all-digital coincidence-detection system implemented in a Field Programmable Gate Array (FPGA) that can cope with the task of generating the high speed trigger for such a camera. The method implemented for coincidence detection is virtually dead-time free and very fast. It is shown the trigger system can process all the events inside the RPC-PET camera in real-time. This will allow a better understanding of the camera and will contribute to its optimization, simplifying significantly the design of its data acquisition system.

KEYWORDS: Trigger concepts and systems (hardware and software); Gamma camera, SPECT, PET PET/CT, coronary CT angiography (CTA); Trigger algorithms

[1] Corresponding author.

doi:10.1088/1748-0221/8/03/C03001

Contents

2013 JINST 8 C03001

1 Introduction

Positron emission tomography (PET) is a non-invasive, in-vivo, functional, molecular imaging modality capable of providing a three-dimensional (3-D) distribution of radio-labelled tracers within living subjects, with great promise for specific identification of cancer, due to its unique ability to sense and visualize increased biochemical changes in malignant compared to healthy tissue before structural changes occur.

One of the possible applications of PET imaging is the studies involving small animals, like transgenic mice and rats. These animals, due to their genetic similarities with humans and easy availability, are useful as experimental models in the development of new drugs, human diseases studies and validation of gene therapies. A considerable effort has been made to develop such a small animal RPC-PET camera. In [1] an experimental setup is described along with results showing the acquisition of images with a resolution of approximately 0.3 mm FWHM. In [2] a trigger system suitable for such a small RPC-PET camera is described.

In the context of human cancer assessment and treatment planning it could be advantageous to do a single bed whole-body scanning of the patient which would contemporaneously look for metastasis and allow for a more appropriate treatment (figure 1). Such whole-body scanning camera would have a prohibitive cost using the standard detector technologies but could be implemented at a very competitive cost using the RPC as a detector.

Efforts to build a whole-body RPC-PET camera are being pursued and significant work at the experimental and simulation level has been carried out [3, 4]. One troublesome feature of such a camera, due to its large area, is the high channel count and the need to implement an appropriate coincidence trigger to reduce the overall amount of data to save and process. It was in the context of the studies on the feasibility of the RPC-PET camera for human whole-body screening that

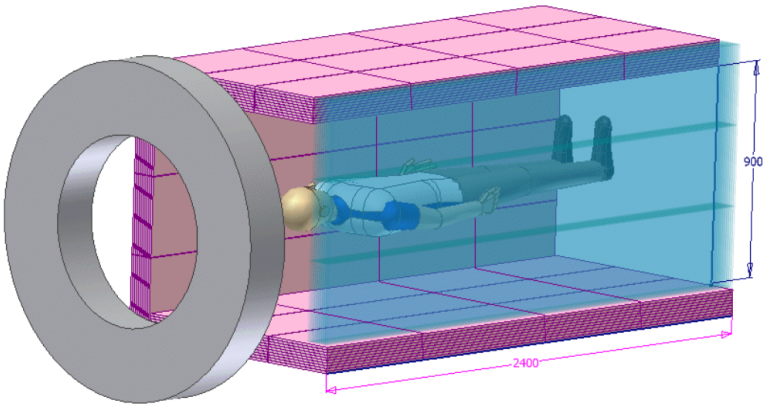

Figure 1. Overall geometry of the camera (shown with an auxiliary CT scanner).

the present work on coincidence detection and intelligent trigger generation was carried out. Our approach is an advancement relative to the usual methods of coincidence detection based on analog discrete implementations (as was done in [1]) or in off-line processing (as in [5]). It is especially useful in cameras with a large number of channels.

2 Design architecture

2.1 Working principle

Each RPC plate in the camera generates a fast hit signal (the RPC time channel) when a photon is detected. This signal is sent to the FPGA, where it is digitized (one-bit digitization). The digitized signal forms a stream of zeros and ones. Each transition from zero to one marks the initial moment of detection of an event in the RPC plate. If the time instant of occurrence of such transitions is known it is possible to compare them across channels and detect events within a specified time window, and generate an appropriate coincidence trigger signal.

By doing all processing inside a single FPGA, using just one clock for digitizing all inputs, the difficult problems of clock synchronization and distribution associated with other solutions using distributed resources are avoided. The time resolution of such a centralized system will depend essentially on the characteristics of the clock used.

2.2 Camera constraints and coincidence validation

Each experimental setup will usually have its own requirements in terms of the time coincidence window (and possibly more advanced information on coincidence validation) that will have to be considered while designing the dedicated coincidence-detection system. The optimal coincidence detection window, due to the geometry of the RPC-PET camera and the large field of view, is expected to be in the nanosecond range. Its exact value will be dependent on the final design of the camera. Nevertheless we expect a tight time window (in the order of a few nanoseconds). It should also be emphasized the large number of RPC plates involved (we are aiming at a number that can reach 100), each one providing a time channel to be checked for coincidences.

2013 JINST 8 C03001

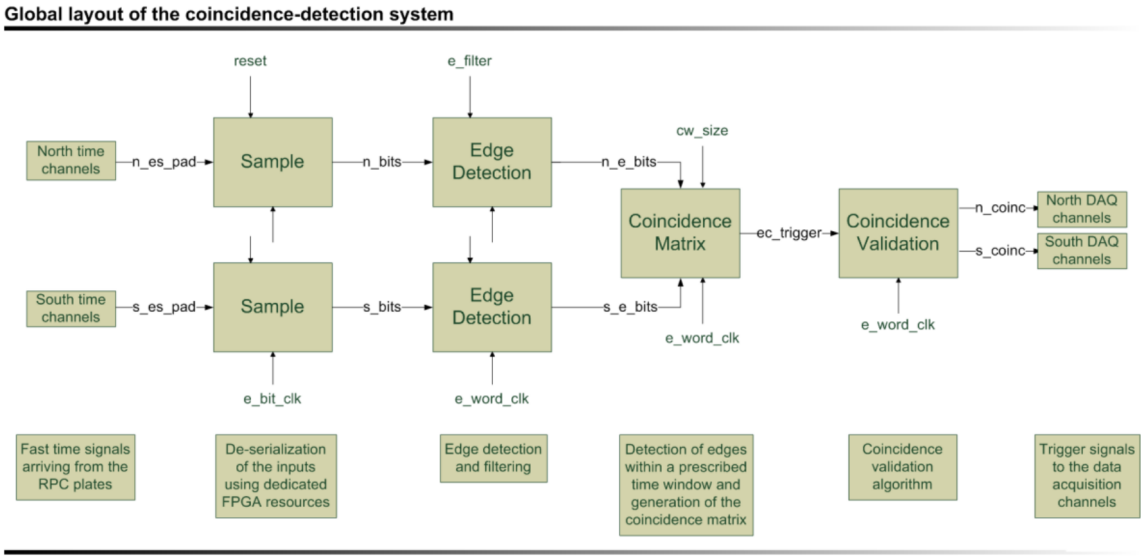

Figure 2. Global layout of the coincidence-detection system.

Another interesting and eventually difficult point is the need to implement geometrically-related validation schemes, again imposed by the large field of view of the camera (current simulation work is being done on defining the best solid angle of acceptance for coincidences, aiming at reducing the overall noise of the reconstructed image). These trigger validation schemes need information on the spatial location of the detectors involved in the coincidence event. One way of obtaining it is to build a table of coincidences involving all time channels. It is then possible to inhibit trigger generation from coincidence events detected by prohibited pairs, specified according to some optimization criteria.

2.3 Conceptual layout of the coincidence-detection system

In the following we will consider two groups of RPC detectors that are to be checked for coincidences: the north group (top of the camera) and the south group (bottom of the camera). Each group of detectors is composed of several RPC plates, each one having its own time channel. Each RPC plate will also produce other slow information, to be read by several data acquisition (DAQ) channels: the use of 12-bit 65 MHz ADCs is foreseen to digitize the information on each of these DAQ channels, with each RPC plate having 16 of them. The slow information, corresponding to the charge induced in the RPC pickup strips by the electron avalanche produced by the interaction of the 511 keV photons resulting from the positron annihilation, is read by charge sensitive amplifiers and used to determine the position of the electron avalanche in the RPC. In the case where a prompt coincidence is detected a trigger signal is sent to the DAQ channels so that data are digitized and eventually sent to the image reconstruction engine.

The time channels are seen as sources of streams of zeros and ones. The state of each time channel is identified by the value measured: if zero the channel is inactive (no event detected in the channel), whereas if one an event was detected and is currently being processed.

The state of the time channels is continuously monitored by the Sample block (figure 2), which samples each time channel (n_es_pad and s_es_pad signals) using a fast clock (e_bit_clk), and creates

2013 JINST 8 C03001

a de-serialized version of the input, producing output words (n_bits and s_bits) that are sent to the Edge Detection block at a lower clock rate (clock e_word_clk).

The Edge Detection block implements a simple edge detection algorithm replacing the row of consecutive 1s in n_bits and s_bits by just the first 1, resulting in the n_e_bits and s_e_bits words, where each 1 indicates the time instant when an event was detected. This block, designed in a general way (can be customized by selecting parameters), supports different word sizes and can optionally filter the input word for a minimum number of consecutive 1s, thereby implementing a kind of electrical noise filter (with width programmed by e_filter).

The Coincidence Matrix block gathers edge information (contained in n_e_bits and s_e_bits) from every time channel and checks for coincidences inside a given coincidence window. In this process every time channel from the north group is checked for coincidences with all time channels of the south group. The time window used is specified by cw_size. The result is a matrix (ec_trigger) with size equal to (the number of north time channels) $\times$ (the number of south time channels), where each line contains the coincidences of the corresponding north channel with all south channels.

The Coincidence Validation block implements the algorithm that validates the detected coincidences. The validated trigger signals (n_coinc, s_coinc) can then be sent to the DAQ channels and the slow data, containing information on the spatial location of the event in the RPC plate, can be saved and/or processed.

The structure of the coincidence-detection system also makes it possible to count the different kinds of events detected (singles, multiple coincidences, coincidences rejected due to solid angle, prompt coincidences). These statistics may prove useful for the image reconstruction. In fact, the singles-based random coincidence estimation method can then be applied, which would allow an improvement in sinogram and image signal-to-noise ratios by approximately 15% when compared with the usual online subtraction of delayed coincidences [6].

3 Implementation and simulation results

3.1 Implementation

The design is completely synchronous and was written in VHDL. We used the de-serialization features of the input pads of the Virtex-5 family of FPGAs in the Sample block of figure 1, resulting in an implementation free of meta-stabilities. This has also the important advantage of reducing the high-speed sampling clock (e_bit_clk, a 550 MHz double data rate (DDR) clock) to the slower e_word_clk word processing clock (a 275 MHz clock in the actual implementation) used by all other blocks. If needed this clock reduction can be further enhanced by increasing the width of the de-serialized words.

The time channel from each RPC plate is binary sampled and de-serialized using the e_bit_clk clock. Each stream of data produced is optionally filtered for noise removal and an edge detection algorithm is run. The edges found are then checked for coincidence detection. In the actual implementation the coincidence window can be selected in increments of 0.9 ns up to 3.6 ns. The coincidences are detected in parallel in all time channels resulting in a 50×50 matrix of coincidences (for a system with 50 north and 50 south time channels). An algorithm to globally validate the coincidences is then applied.

2013 JINST 8 C03001

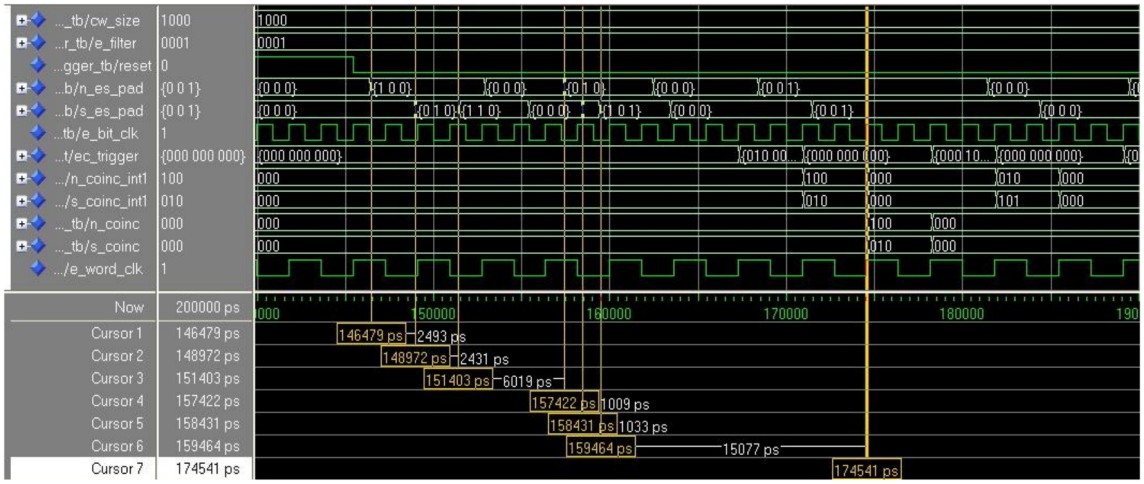

Figure 3. Three north and three south time channels, 3.6 ns coincidence window. A first set of transitions shows events in time channels n_es_pad(3) and s_es_pad(2) that are inside the coincidence window and trigger signals are generated and sent in less than 30 ns to the intervening RPC plates (signals n_coinc(3) and s_coinc(2). A second set of transitions are rejected due to multiple events detected inside the coincidence window.

The method implemented for coincidence detection is virtually dead-time free and very fast. In the actual implementation the data words produced by sampling the time channels are scanned every 3.6 ns and the coincidence matrix is refreshed at this rate. A trigger signal can be sent to the RPC plates originating the coincidences in less than 30 ns after the fast hit signals were received, allowing the collection of the slow data (containing the information on the position of the event in the RPC plate) just in the plates involved in the coincidence event.

3.2 Simulation results

Several simulation results, obtained using ModelSim and post-placement and route models, are shown. For ease of visualization only results from a system composed of 3 north and 3 south time channels are initially shown and no input filtering is performed. Similar signals are grouped in arrays, as the input signals arriving from the north time channels and received as inputs in the FPGA under the name n_es_pad. For instance, in a system composed of 3 north time channels there are three input signals named n_es_pad(3), n_es_pad(2) and n_es_pad(1). Figure 3 was obtained with a coincidence window of 3.6 ns while in figure 4 the coincidence window was 1.8 ns. The stimuli were the same in both cases.

In the following it is helpful to consider figure 3.

The input signals arriving from the time channels are DDR sampled at the pads of the FPGA (n_es_pad and s_es_pad signals) and de-serialized at the pad level using the 550 MHz clock e_bit_clk. The resulting words are then processed internally at the half-speed, non-DDR, e_word_clk clock. The edges of the de-serialized signals are found and checked for coincidences and results are saved in the coincidence matrix ec_trigger. Each line of this matrix shows the coincidences of the corresponding north time channel with all south time channels. Time cursors show the time interval between the first transitions of the input signals. Initially n_es_pad(3) changes state, followed ap-

2013 JINST 8 C03001

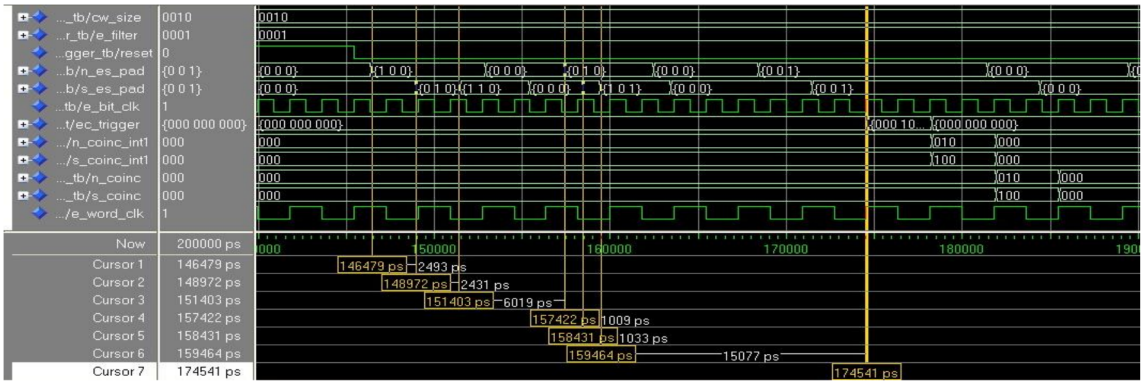

Figure 4. Three north and three south time channels, 1.8 ns coincidence window. The first set of transitions generates no coincidences as they are outside de coincidence window. The second set of transitions generates coincidence trigger signals n_coinc(2) and s_coinc(3) that are sent to the corresponding RPC plates.

proximately 2.5 ns later by s_es_pad(2), and approximately 2.4 ns later s_es_pad(3) also changes state. The last cursor indicates the first output trigger signals generated: a coincidence was detected and validated between input time channels n_es_pad(3) and s_es_pad(2) due to the first set of transitions described. This results in the generation of the output coincidence trigger signals n_coinc(3) and s_coinc(2): they can now be sent to the intervening RPC plates to allow acquisition of the slow data generated by the events.

As a first algorithm for random event suppression the trigger signals are inhibited in the case where more than two events are detected inside the same coincidence window. This happens in the next set of input transitions. First n_es_pad(2) becomes high; approximately 1 ns later s_es_pad(3) also becomes high; after approximately another 1 ns s_es_pad(1) becomes also high. Two events are detected in the south channels inside the 3.6 ns coincidence window, as can be seen in s_coinc_int1 (this is an internal signal to help making decisions based on the coincidence matrix), and no output trigger signals are generated. A more realistic algorithm would include rejecting events that lay inside the correct time window but are detected outside a maximum acceptance solid angle (e.g., events detected near the patient head and foot). This kind of algorithm is very easy to implement. In fact, having generated the coincidence matrix one knows exactly the detectors involved in the events and it is possible to inhibit coincidences generated from "not allowed" detector pairs simply by masking. This will prevent coincidence trigger signals to be sent to the intervening DAQ channels.

Figure 5 shows simulation results for a system with 100 time channels (50 north and 50 south channels) with a coincidence window width of 3.6 ns. A first transition is shown in n_es_pad(50) followed by transitions in s_es_pad(49) and s_es_pad(48). Less than 25 ns later coincidences are identified between channels n_coinc(50) and s_coinc(49): the signal in s_es_pad(48) arrives approximately 5 ns after the transition in n_es_pad(50) and is not inside the coincidence window.

Another set of transitions can be seen (n_es_pad(49), s_es_pad(50), s_es_pad(46)). As the transitions are inside the coincidence window (they are in fact 1 ns apart from each other) coincidences are detected between channel n_coinc(49) and channels s_coinc(50) and s_coinc(46). Depending on the global validation algorithm implemented the coincidence could be discarded as probably a random event occurred at the same time.

2013 JINST 8 C03001

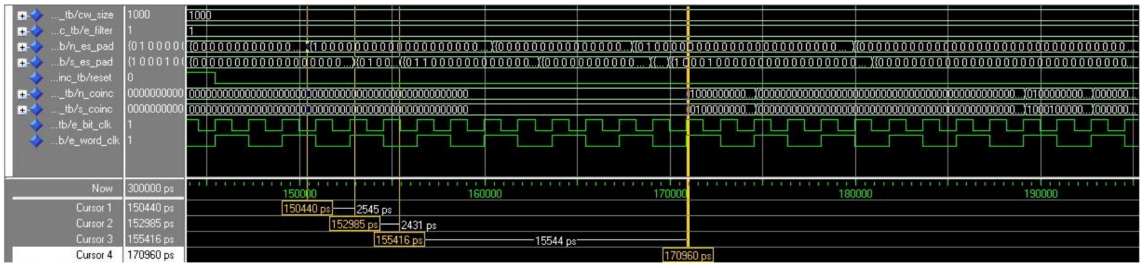

Figure 5. A system with 100 time channels, 3.6 ns coincidence window. Coincidence trigger signals are generated due to events inside the coincidence window.

3.3 Throughput of the coincidence-detection system

As can be deduced from the simulations shown the operation of the coincidence trigger depends on the ability to detect the transition marking the initial instant of detection of an event in the detectors. The maximum allowed event rate the system can cope with is limited only by the need of the input signals arriving at the FPGA be sampled low (before an event occurs), then high (when an event is detected) and then low again before a new event can be detected. The present system can easily cope with, for instance, a 100 MHz event rate, simultaneous in all channels, provided the input signals arriving at the FPGA could be sampled low-high-low during a 10 ns time interval. In comparison the total activity inside the RPC-PET camera is expected to be under the usual 10 mCi in available tomographs. The 10 mCi activity will generate a total event rate of around 3.7×10^8 disintegrations per second that, from the point of view of the trigger system, could be arriving at just one RPC plate and still be effectively processed.

4 Conclusion

The proposed solution can cope with the need to generate very fast and intelligent coincidence trigger signals for systems with a large number of channels and high event rates. Its easy programmability allows implementation of intelligent dedicated triggers, opening new avenues for on-line data reduction, with immediate benefits in terms of reducing the complexity of the overall data acquisition system of the camera and the time taken for image reconstruction.

Acknowledgments

This work was financed by FCT under Contract PTDC/SAU-BEB/104630/2008.

References

[1] A. Blanco et al., *Very high position resolution gamma imaging with resistive plate chambers*, *Nucl. Instrum. Meth.* **A 567** (2006) 96.

[2] F.M.C. Clemencio, C.F.M. Loureiro and J. Landeck, *Online trigger processing for a small-animal RPC-PET camera*, *IEEE Trans. Nucl. Sci.* **58** (2011) 1766.

[3] M. Couceiro et al., *RPC-PET: status and perspectives*, *Nucl. Instrum. Meth.* **A 580** (2007) 915.

[4] A. Blanco et al., *Efficiency of RPC detectors for whole-body human TOF-PET*, *Nucl. Instrum. Meth.* **A 602** (2009) 780.

[5] D.P. McElroy et al., *A true singles list-mode data acquisition system for a small animal PET scanner with independent crystal readout*, *Phys. Med. Biol.* **50** (2005) 3323.

[6] D. Brasse et al., *Correction methods for random coincidences in fully 3D whole-body PET: impact on data and image quality*, *J. Nucl. Med.* **46** (2005) 859.

2013 JINST 8 C03001